Autophagy induces hair follicle stem cell activation and hair follicle regeneration by regulating glycolysis

Pingping Sun
Southern Medical University Nanfang Hospital
Zhan Wang
Southern Medical University Nanfang Hospital
Sixiao Li
Southern Medical University Nanfang Hospital
Shizhao Liu
Southern Medical University Nanfang Hospital
Yuyang Gan
Southern Medical University Nanfang Hospital
Zhen Lin
Southern Medical University Nanfang Hospital
Hailin Wang
Southern Medical University Nanfang Hospital
Zhexiang Fan
Southern Medical University Nanfang Hospital
Qian Qu
Southern Medical University Nanfang Hospital
Zhiqi Hu
Southern Medical University Nanfang Hospital
Kaitao Li
Southern Medical University Nanfang Hospital
Yong Miao (miaoyong123@i.smu.edu.cn)
Southern Medical University Nanfang Hospital https://orcid.org/0000-0003-4254-0673

Research Article

Keywords: Hair follicle stem cells, Autophagy, Glycolysis, Hair follicle regeneration

Posted Date: June 5th, 2023

DOI: https://doi.org/10.21203/rs.3.rs-2932991/v1

Version of Record: A version of this preprint was published at Cell & Bioscience on January 5th, 2024. See the published version at https://doi.org/10.1186/s13578-023-01177-2.

Abstract

Background

Hair follicle stem cells (HFSCs) are usually in a resting state and are activated during the transition from telogen to anagen phases to ensure that the hair follicle enters a new cycle. Macroautophagy/autophagy regulates stem cell metabolic behavior in tissues, and changes in HFSC metabolism directly affect HFSC activation and maintenance. However, the role of autophagy in the regulation of HFSC metabolism and function remains unclear.

Methods

Back hair of mice at different hair follicle cycle stages was collected, and immunofluorescence staining was used to detect changes in HFSC autophagy levels in the hair follicle cycle. Mouse and human hair follicles were treated with rapamycin (Rapa, an autophagy activator) and 3-methyladenine (3-MA, an autophagy inhibitor). The effects of autophagy on the hair follicle cycle and HFSC were investigated by imaging, cell proliferation staining, and HFSC-specific marker staining. The influence and mechanism of autophagy on HFSC metabolism were explored by RNA sequencing, real-time polymerase chain reaction (PCR), immunohistochemical staining, and lactate and glucose detection. Finally, the influence of autophagy-induced glycolysis on HFSC and the hair follicle cycle was verified by proliferation, stem cell characteristics, and in vivo functional experiments.

Results

The HFSC autophagy level in hair follicles was highest during the transition from the telogen to the anagen phase. The inhibition of autophagy with 3-MA led to early entry into the catagen phase and a prolonged telogen phase, whereas Rapa promoted autophagy and hair growth. Autophagy activated HFSC by increasing the activity of HFSC lactate dehydrogenase (Ldha) and lactate production and transforming HFSC metabolism into glycolysis. The inhibition of Ldha expression counteracted the effects of autophagy.

Conclusions

These results demonstrated that autophagy activated HFSC by promoting the transition from HFSC metabolism to glycolysis, ultimately initiating the hair follicle cycle and promoting hair growth.

Introduction

Hair follicles undergo anagen, catagen, and telogen phases, thereby forming a cycle of hair growth, shedding, and regrowth. Hair follicle stem cells (HFSCs) are located in the bulge area of hair follicles and

are characterized by the expression of various immunohistochemical markers, including cytokeratin-15 (CK15) and cytokeratin-19 (CK19). HFSCs undergo activation and quiescence in a manner that is highly synchronized with the hair follicle cycle[1, 2]. A prolonged telogen phase and hair miniaturization caused by HFSC activation disorders among the pathological bases of alopecia, including androgenic alopecia (AGA)[3, 4]. HFSC activation is regulated by various internal and external mechanisms. Recent studies have found that compared to other epidermal cells, HFSCs tend to utilize glycolytic metabolism to produce more lactate, a metabolic characteristic that allows them to respond quickly to hair follicle growth stimulation[5]. The transition from HFSC to outer root sheath (ORS) progenitor cells involves the activation of oxidative phosphorylation and the entry of glutamine into the tricarboxylic acid (TCA) cycle. Importantly, some ORS progenitor cells can be reprogrammed by inhibiting the metabolic transition from glycolysis to oxidative phosphorylation (OXPHOS) and glutamine metabolism in the early development of the HFSC lineage and restoring stem cell status, thus forming a new HFSC ecological niche[6]. However, the regulation of metabolic pathways in HFSCs has not yet been reported.

Autophagy is an intracellular degradation system that transmits cytoplasmic substances to lysosomes for degradation and plays various roles in the physiological processes of cell disease. Orhon et al. used a three-dimensional organoid system to evaluate the effect of autophagy on mouse salivary gland stem cells (SGSCs), in which enhanced autophagy induced SGSCs activation and played an important role in maintaining the self-renewal characteristics of SGSCs[7]. Several studies have shown that autophagy regulates cellular metabolism. For example, autophagy maintains mitochondrial function and quantity in hematopoietic stem cells, leaving cells metabolically at low levels of OXPHOS, while impaired autophagy leads to excessive activation of hematopoietic stem cells and senescence phenotypes[8].

Recent studies have shown that -ketoglutarate (-KG) and -ketobutyrate (-KB), as well as the prescription drugs rapamycin and metformin, increase follicle autophagy by affecting mTOR and AMP2 signaling, facilitating the early entry of hair follicles into the resting phase[9]. However, Parodi et al. used an in vitro human hair follicle organ culture model to demonstrate that anti-hair loss products with autophagic effects can significantly enhance the autophagy of hair follicle cells and prolong hair follicle growth[10]. However, the effects of autophagy on HFSC metabolism and function during the follicular cycle remain unclear. Understanding the mechanism of autophagy in HFSC metabolism is important for treating or preventing hair loss due to the failure of HFSC activation.

In this study, we measured the autophagy levels of HFSC in different hair follicle cycles and investigated the effects of autophagy on the hair follicle cycle and HFSCs. We also investigated the effects and mechanisms of autophagy on HFSC metabolism, and whether autophagy affects HFSC function and the follicular cycle by regulating cellular metabolism.

Results

3.1 Increased autophagy level in HFSC during the transition phase (telogen-anagen transition)

The cellular activity differed significantly between resting and growing hair follicles. During the telogen phase, hair follicle stem cells rest until they are activated and proliferate upon receiving growth stimulation signals (Supplementary Fig. 1). To investigate the level of HFSC autophagy in different hair follicle cycles, we performed co-localization assays of the autophagy markers LC3B, P62, and HFSC-specific marker K15 on the dorsal skin of mice in the early telogen phase (50 days after birth), mid-late telogen phase (63 days after birth), telogen-anagen phase transition (77 days after birth), and anagen phase (84 days after birth). Fewer LC3B-positive sites in HFSC were observed in the early and mid-late telogen phases; the numbers increased briefly in the transition phase and then decreased after entering the anagen phase; whereas P62 levels decreased in the transition phase, corresponding to LC3B-positive sites (Fig. 1A-C). HFSC autophagy was induced during the telogen-anagen phase transition of hair follicles and returned to lower levels after entering the anagen phase, and the level of HFSC autophagy was consistent with hair follicle cycle changes, suggesting that changes in HFSC autophagy may play an important role in the critical process of hair follicles entering the anagen phase from the telogen phase.

3.2 Autophagy regulates the hair follicle cycle and HFSC activation

To investigate the effect of transitional autophagy upregulation on the hair follicle cycle, we selected mice treated with hair removal and drug injection in the mid-late telogen phase (9th–10th weeks after birth). Immunofluorescence staining of hair follicles from mice 1 day after drug treatment showed fewer HFSC LC3B-positive sites in the 3-MA group and significantly more HFSC LC3B-positive sites in the Rapa group compared to the control group, while HFSC p62 levels increased in the 3-MA group and decreased in the Rapa group, thus demonstrating that 3-MA and Rapa effectively inhibited and promoted HFSC autophagy, respectively (Fig. 2A-C). We first explored the effect of 3-MA alone on the hair follicle cycle, photographed on days 0, 7, 9, and 11 after drug treatment, and analyzed the skin hair growth conditions using imaging software. On day 7, we observed melanosis in both the 3-MA and control groups; however, the mice in the 3-MA group had a much lighter skin color compared to the control group. On day 11, the melanosis rate in the control group was 1.57 and 1.78 times that of the telogen period, respectively, while the melanosis rate in the 3-MA group was only 1.29 and 1.42 times that of the telogen period (Fig. 2D and 2E). This indicated that autophagy inhibition delayed the telogen-anagen phase transition in mouse hair follicles. We further investigated whether autophagy promoted the early entry of hair follicles into the anagen phase in mice. Surprisingly, on day 11, mice in the Rapa group had regained almost intact hair, whereas most of the hair follicles in the 3-MA group remained in the telogen phase (Fig. 2F and 2G). Hematoxylin and eosin (H&E) staining of the skin confirmed these findings (Fig. 2H). To investigate whether autophagy had an activating effect on HFSCs, we performed Ki67 staining of hair follicles of mice 7 days after treatment. On day 7, more HFSCs in the bulge area of the Rapa group showed proliferation, while fewer HFSCs in the control group and almost none in the 3-MA group showed

proliferation (Fig. 2I). Previous studies have reported that plucking hair from the backs of mice can unify the hair follicle cycle and induce the early anagen phase[11]. On the first day after hair plucking, we observed increased HFSC LC3B expression on the dorsal side of mice, and more positive points for HFSC LC3B in the chloroquine (CQ)-treated group compared to the hair plucking group, indicating active HFSC autophagic flux (Supplementary Fig. 2) and suggesting that enhanced HFSC autophagy may be one of the mechanisms for the early entry of hair follicles into the anagen phase after hair plucking.

To evaluate whether autophagy also plays a role in regulating the cycle and activating HFSCs in human hair follicles, we used the experimental method of *in vitro* organ culture of human hair follicles to observe the effect of autophagy on hair follicles in close proximity to the physiological microenvironment and histomorphology. Human hair follicles were treated with Rapa (1 nM) and 3-MA (5 uM) for 6 h. We observed a decrease in HFSC LC3B-positive sites and an increase in p62 levels in the 3-MA group, and an increase in HFSC LC3B-positive sites and a decrease in p62 levels in the Rapa group, demonstrating that drug treatment effectively affected HFSC autophagy levels (Fig. 3A-C). Next, we morphologically assessed the change in the length of each hair follicle after drug treatment for 1–7 days and the stage of the hair follicle cycle on day 7. We observed that 3-MA retarded hair shaft growth, whereas rapamycin significantly promoted it (Fig. 3D). On day 7, approximately 30% of the control follicles were in the anagen phase and < 20% of the 3-MA group were in the anagen phase, whereas > 50% of the Rapa-cultured follicles were still in the anagen phase (Fig. 3E and 3F). To further verify the effect of autophagy on HFSC, we compared HFSC proliferation and the expression of the HFSC marker K15 after 3 days of culture under different treatments. The percentage of HFSC and daughter Ki67 + cells significantly increased in Rapa-treated hair follicles, whereas 3-MA-treated hair follicles had fewer HFSCs and daughter Ki67 + cells than the control group (Fig. 3G and 3H). Drug treatment appeared to not affect HFSC K15 expression in the bulge region; however, Rapa significantly promoted K15 expression in HFSC daughter cells above the hair bulge (Fig. 3I). Because K15 is a marker of stem cell-specific expression in the bulge region, the restoration of K15 expression in daughter cells above the bulge was considered to restore stem cell properties.

In summary, autophagy upregulation activated HFSC, thus promoting hair follicle cycle activation in mice and prolonging the anagen phase of human hair follicles, prolonging the telogen phase of hair follicles in mice, and causing human hair follicles to enter the catagen phase earlier. Therefore, autophagy plays an important role in HFSC activation and hair follicle cycle regulation.

3.3 Induction of autophagy promotes a shift in HFSC metabolism toward glycolysis

Previous studies showed that autophagy contributes to the maintenance of glycolytic metabolism in hematopoietic stem cells and that impaired autophagy leads to abnormal hematopoietic stem cell maintenance and function[12] .To investigate the effect of autophagy on HFSC metabolism, we first examined the effect of different concentrations of drug treatment on cell activity and proliferation using live-dead staining and CCK8 reagent. HFSCs were extracted as previously described[13] and assayed when

the cell fusion reached 80%. After 24 h of drug treatment, the cell activities did not differ significantly, but 3-MA inhibited cell proliferation, while Rapa promoted cell proliferation in a concentration-dependent manner, with no effect on cell proliferation at 0.05 nM and 2.5 nM, while 0.5 nM Rapa promoted cell proliferation most significantly (Supplementary Fig. 3A and 3B).

We also examined the cellular autophagy levels after treating HFSCs with Rapa (0.5 nM) and 3MA (5 mM) for 6h. Consistent with the previous results, we observed an increase in LC3B-positive sites, weakened P62 expression, and increased autophagic flow in HFSCs in the 0.5 nM Rapa group. In the 3-MA group, we observed a decrease in LC3B-positive sites, enhanced P62 expression, and weakened autophagic flow (Fig. 4A-C). Next, we performed a transcriptome sequencing analysis of HFSC after Rapa treatment for 24 h. Both KEGG and GO enrichment pathway analyses showed significant changes in glycolytic metabolism in the enriched top pathway (Fig. 4D-E). To investigate the relationship between autophagy and HFSC glycolysis, we collected HFSC culture supernatants after 18 h and 24 h of treatment with 3-MA and different concentrations of Rapa and measured the lactate and glucose concentrations in the supernatants. The results showed that Rapa promoted glucose consumption and lactate production in HFSCs, with 0.5 nM Rapa having the most significant and rapid effect on HFSCs; in contrast, 3-MA significantly inhibited glucose consumption and reduced lactate production in HFSCs (Fig. 4F and 4G). We also found that the intracellular lactate concentration in HFSCs after Rapa treatment was 3.75 times higher than that after 3-MA treatment (Fig. 4H). These results suggested that autophagy induction can promote a shift in HFSC metabolism to glycolysis and increase glucose consumption and lactate production in HFSCs.

3.4 Autophagy promotes Ldha expression and up-regulates Ldha activity in HFSCs

Previous studies confirmed the regulatory role of autophagy on cellular glycolysis, a role that may be mediated by regulating the expression of glycolytic metabolic enzymes[13–15]. Therefore, to investigate the regulatory mechanism of autophagy in HFSC metabolism, we examined the expression of key glycolytic enzymes in HFSCs by real-time PCR. We found that Rapa and 3-MA upregulated and 3-MA inhibited Ldha expression in HFSCs, respectively (Fig. 5A and 5B). To investigate the role of Ldha in autophagy-induced HFSC glycolysis, we transfected HFSCs were transfected with *Ldha* siRNA for 48 h to reduce Ldha expression. Real-time PCR to examine the knockdown effect of si-*Ldha* showed that si-*Ldha* effectively downregulated Ldha expression (Fig. 5C)[15]. When autophagy was induced by Rapa, Ldha knockdown reduced the rates of lactate production and glucose consumption in HFSCs (Fig. 5D). We then verified the role of autophagy in promoting Ldha expression in human hair follicle organ cultures *in vivo*. Human hair follicles were treated with Rapa and 3-MA for 24 h before Ldha expression was detected by immunohistochemical staining. Rapa significantly promoted human hair follicle Ldha expression in HFSCs, whereas 3-MA inhibited Ldha expression in HFSCs (Fig. 5E). We verified these findings *in vivo* by injecting the experimental group drug and the control group solvent into the dorsal surface of C57 mice and assayed 24 h later. Consistent with the results of the human hair follicle assay, Rapa promoted Ldha

expression in mouse dorsal hair HFSCs, whereas 3-MA inhibited Ldha expression in HFSCs (Fig. 5F). In addition, differential gene analysis of the glycolytic pathways revealed that LDHAL6A was the glycolytic enzyme with the most significant changes in RapA-treated HFSCs (Fig. 5G and 5H). Since LDHAL6A may be positively correlated with Ldha activity, we lysed the drug-treated cells and subjected the cell lysates to an enzymatic assay similar to the colorimetric assay. The results showed that Rapa increased HFSC Ldha activity (Fig. 5I). These results suggest that autophagy shifts HFSC metabolism toward glycolysis by promoting Ldha expression and increasing Ldha activity in HFSCs.

3.5 Autophagy activates HFSC and induces hair growth by promoting glycolysis

To further investigate the effect of autophagy-induced upregulation of Ldha expression on HFSCs and the hair follicle cycle, we performed EdU staining of HFSCs and found that Rapa promoted HFSC proliferation, whereas transfection with si–*Ldha* significantly impaired the promotion of HFSC proliferation (Fig. 6A and 6B). Furthermore, a clone formation assay to assess the effect of autophagy on HFSC proliferation showed that Rapa significantly promoted HFSC colony formation and increased the number of cells in individual HFSC colonies, while transfection with si-*Ldha* inhibited the promoting effect of Rapa on HFSC colony formation (Fig. 6C and 6D). To investigate whether autophagy overactivates HFSCs, leading to the loss of their properties, we measured the number of HFSC K15 + and K19 + cells by immunofluorescence staining. Rapa significantly increased the number of K15 + and K19 + HFSC(Fig. 6E and 6F), with two-fold more K15 + HFSC than the control and 5.25 times more Rapa + si-*Ldha* group, while K19 + HFSC were 1.6 times more than the control and 4 times more Rapa + si-*Ldha* group (Fig. 6G and 6H). These results suggest that autophagy activates HFSCs by upregulating Ldha expression and promoting HFSC proliferation while maintaining at least a portion of the stem cell properties of HFSCs without leading to HFSC overactivation.

Finally, to investigate whether autophagy-induced upregulation of LDHA expression is a key pathway for autophagy to alter the hair follicle cycle, we injected the backs of mice with control solvent, Rapa solution, and Rapa + si-*Ldha* solution every other day and recorded hair follicle coverage on days 0, 7, 9, and 11 after drug treatment. We analyzed the hair growth area using image software. On day 11, the hair follicles of mice treated with Rapa had largely all entered the anagen phase, whereas most of the hair follicles of Rapa + si-*Ldha*-treated mice were still in the telogen-anagen phase transition, indicating that transfection with si-*Ldha* significantly inhibited the effect of Rapa on promoting hair follicle growth (Fig. 7A-C). Human hair follicle organs were treated identically, and human hair follicles were cultured in William's E conditioned medium containing control solvent, Rapa, and Rapa + si-*Ldha*, and the change in length per follicle after 1–7 days of treatment and the stage of follicular cycle at day 7 were assessed. At day 7, the proportion of follicles in the Rapa + si-*Ldha* group during the anagen phase was reduced by 10%-30%, the proportion of follicles in the telogen phase was increased by 20%-30%, and follicle elongation was reduced by approximately 10% compared to follicles treated with Rapa alone (Fig. 7D-F), indicating that

transfection with si-*Ldha* significantly inhibited the effects of Rapa in extending follicle anagen and promoting follicle growth.

In summary, these data suggested that autophagy activates HFSCs by upregulating Ldha expression to promote glycolysis, thereby regulating the hair follicle cycle and promoting hair growth.

Discussion

Hair follicle stem cells (HFSCs) are adult stem cells that can self-renew and differentiate into many different cell types. During the hair cycle, HFSCs are activated during the anagen phase, then start to proliferate and differentiate to replenish the epidermal components of the hair follicle (e.g., hair matrix cells), maintain quiescence, and stop hair follicle growth. In pathological states such as androgenetic alopecia, HFSC activation is impaired, leading to a shortened anagen phase and a prolonged telogen phase, resulting in alopecia. Therefore, it is important to study the mechanisms that regulate HFSC activation for the treatment of alopecia.

Autophagy is the process by which cells wrap products to be degraded through the membrane and form autophagic vesicles that are transported to lysosomes for degradation, thereby maintaining the metabolic homeostasis of cells and regulating the activation of stem cells[16]. In normal resting hair follicles, the level of autophagy decreases and remains low, while it is enhanced when entering the anagen phase; inhibition of autophagy causes the hair follicle to enter the catagen phase earlier[9, 10], indicating the importance of autophagy for initiating the normal hair follicle cycle and hair regeneration in the physiological state. In a mouse model of baldness, hair follicle autophagy was inhibited, and the induction of autophagy attenuated the baldness phenotype, whereas the prevention of autophagy promoted disease development[17]. Parodi et al. identified hair matrix cells as possible target cells for autophagy. However, hair matrix cells, as rapidly dividing cells, undergo apoptosis quickly, and there remain still limitations to treating hair loss by regulating hair matrix cells and thus hair loss. In contrast, HFSCs, which are progenitors of hair matrix cells and seed cells for hair follicle regeneration, can exist stably for a long time. Therefore, autophagy, an important physiological function for cells to respond to external stimuli and maintain long-term homeostasis, is also present in HFSCs. Our study is the first to report that autophagy also occurs in HFSCs and that the level of autophagy in HFSCs is consistently low during the telogen and anagen phases and increases significantly during the telogen-anagen phase transition, which is consistent with the hair follicle cycle, suggesting the important role of autophagy in promoting HFSC activation, thus initiating the hair follicle cycle (Fig. 1). To further clarify the regulatory role of autophagy in HFSC activation, 3-MA and Rapa were used to pharmacologically modulate autophagy. The data showed that, under normal physiological conditions, autophagy inhibition impeded follicular cycle progression, whereas autophagy stimulation was sufficient to activate HFSCs, promote early HFSC proliferation, and ultimately advance the hair follicle anagen phase (Fig. 2). Furthermore, to explore whether the regulation of HFSC activation by autophagy is conserved in humans, we investigated the effects of autophagy on HFSCs and the hair follicle cycle under physiological tissue morphology and microenvironment using a human hair follicle organ culture model. We found that the induction of

autophagy promoted human HFSC proliferation and prolonged the anagen phase of hair follicles (Fig. 3), suggesting that autophagy-activated stem cells are also conserved in human hair follicles. Unexpectedly, we also found that autophagy induction restores some of the stem cell characteristics of HFSCs (Fig. 3). Although previous studies reported that autophagy is effective in activating and restoring the stem cell properties of some HFSC progeny cells, our study did not determine whether autophagy plays a different role in HFSCs and their progeny cells, which requires further research.

Metabolism is an important target of autophagy-regulated stem cell functions[18]. Glycolysis, lipid metabolism, and glutamine metabolism can affect HFSC activation in hair follicles[5, 19]. However, whether it is possible to metabolically regulate HFSC activation via autophagy and which metabolic pathways play specific roles remain unknown. To further explore the mechanism by which autophagy regulates HFSC activation, we sequenced the transcriptome and found that autophagy may be related to glycolysis. Further experiments confirmed that autophagy could regulate HFSC glycolysis (Fig. 4–5) by upregulating Ldha expression and activity and promoting lactate production in HFSCs. Flores et al. suggested that HFSCs tend to be more glycolytic than other skin epidermal cells and that increased production of lactate through Ldha appears to be key to activating HFSCs[5]. By knocking out Ldha, we identified the major role of upregulated glycolytic metabolism in autophagy, promoting HFSC activation and the early entry of hair follicles into the anagen phase. In addition, transcriptome data analysis revealed that the glycolytic enzyme LDHAL6A may be a key target of autophagy in promoting HFSC activation (Fig. 5G and 5H). Further studies are required to investigate the mechanisms by which autophagy regulates glycolysis in HFSCs. In addition, owing to metabolic changes and cell remodeling, further investigation is needed to determine whether autophagy includes other types of autophagy, such as chaperone-mediated autophagy or mitophagy[20, 21]. Since autophagy plays an important role in preventing senescence and regulating sebaceous gland function, the effects of autophagy on other constituent cells of hair follicles must be explored.

In conclusion, we found that autophagy activated HFSCs and regulated the hair cycle to promote hair growth by upregulating Ldha expression and activity in HFSCs, resulting in increased HFSC lactate production and a shift in HFSC metabolism toward glycolysis. Moreover, pharmacological therapeutic interventions at the autophagy level promoted HFSC activation and restored the stem cell properties of some progeny cells. These results highlighted autophagy as a novel target for activating HFSCs and regulating the hair cycle to treat human hair loss.

Conclusions

HFSC autophagy level in hair follicles was highest during the transition from the telogen to the anagen phase. Furthermore, autophagy activated HFSC by promoting the transition from HFSC metabolism to glycolysis, ultimately initiating the hair follicle cycle and promoting hair growth.

Materials and Methods

Animals

C57BL/6J female mices (7–8 weeks) were purchased from the Experimental Animal Center of Southern Medical University (Guangzhou, China) and were fed under specificpathogen-free conditions. The animal experiments were approved by

the Animal Research Committee, Southern Medical University (Guangzhou, China). All mice studies were conducted under the instructions and permissions of the Animal Care and Use Committee at the International Medical Center.

Immunocytochemistry and Immunohistochemistry

Back skins were harvested from mid-dorsal areas. Then fixed Back skins in 10% formalin solution (Sigma) overnight and dehydrated for embedding in paraffin. 5um paraffin sections were being used in hematoxylin/eosin staining or other staining. Cells were seeded (1 × 104 cells per well) in 24-well plates and cultured until approximately 50% confluency. Then cells were fixed in 4% paraformaldehyde and permeabilized with 0.1% Triton X-100 (Solarbio) in PBS for 10 min at room temperature. Further, the sections or cells were blocked with 3% BSA and incubated with antibodies in 1% BSA for 2h at room temperature. The antibodies used for IHC or IF included: K15 (1:200, Abcam), K19 (1:200, Abcam), LC3B (1:200,proteintech), P62 (1:200,proteintech), Ldha (1:200,proteintech) antibodies. The samples were incubated with the following fluorescence-labeled secondary antibodies in the dark for 1 h at room temperature. Cy3 anti-mouse secondary antibodies (1:500, Beyotime, China), Goat Anti-Rabbit lgG AF 594 (1:200, Abmart), Goat Anti-Rabbit lgG AF 488 (1:200, Abmart) .The nuclei were stained with DAPI (Life T echnologies, USA) prior to imaging with a confocal laser scanning microscope.20–30 pictures were collected using 20x or 40x objectives. Image processing was using ImageJ/Fiji software.

Hair follicles culture

The hair follicles were cultured in 24-well plates with Williams’E medium supplemented with insulin, hydrocortisone, l-glutamine and Penicillin-Streptomycin Solution at 37°C in a 5% CO2 atmosphere. Hair follicles were treated with control, 5uM 3-MA or 1nM Rapa on day1.The elongation of each HF were recorded for consecutive 7 days and hair cycle stage were recorded on day7 (ten hair follicles were analyzed each experiment). The data were obtained from three independent experiments.

Culturing of HFSCs

The bulge of the hair follicle between the isthmus and the upper part of the hair was separated and the HFSCs were cultured as described before[]. Briefly, the isolated bulge tissue was treated with 0.1% Dispase for 20 min and the dermis were separated. The hair shift was treated with 0.025% trypsin(Gibco, Gaithersburg, MD, United States) for 5–6 min at 37◦C. The cell suspension was filtered through a 70 μm filter(Corning, Corning, NY, United States)and centrifuged at 1000r for 3 min. Finally the cells were seeded in six-well plates and cultured in KGM Gold Bulletkit (Lonza,Switzerland) at 37°C in a 5% CO2

atmosphere. Once the cells reached a confluency of 80% ,cells were harvested with 0.25% trypsin, split at a 1:2 ratio, and maintained in KGM Gold Bulletkit.

Cytotoxicity Assay

The HFSCs were cultured in black 96-well plates for 24 h. The culture medium was replaced with 5uM 3-MA or 0.05,0.1,0.5,1,2.5nM Rapa or PBS control KGM for 24 h. The cytotoxicity of 3-MA and Rapa was examined using the (Calcein/PI Cell Viability/Cytotoxicity Assay Kit (Beyotime, China) according to the manufacturer's instructions. The percentage of live cells were measured using a microplate reader (Thermo Fisher, America). Five replicates were analyzed.The data were obtained from three independent experiments.

Cell Proliferation Assay

Cell Proliferation of HFSCs treated with 5uM 3-MA or 0.05,0.1,0.5,1,2.5nM Rapa or PBS control for 24 h was measured using the Cell counting kit-8 (CCK-8; Dojindo Molecular Technologies) according to the manufacturer's protocol (five replicates were analyzed).The data were obtained from three independent experiments.The effect of control,Rapa and Rapa + si-Ldha on HFSC proliferation was examined using the EdU labeling assay according to the manufacturer's protocol. The cells were examined by fluorescence microscope (IX73 FL, Olympus).Image processing was using the ImageJ/Fiji software (three pictures were analyzed). The data were obtained from three independent experiments.

RNA-sequencing (RNA-seq)

Total RNA of the control and Rapa-treated (0.5nM) HFSCs were extracted from three independent experiments together using the Trizol reagent (Invitrogen, CA, USA) according to the manufacturer's protocol. RNA purity and quantification were evaluated using the NanoDrop 2000 spectrophotometer (Thermo Scientific, USA). RNA integrity was assessed using the Agilent 2100 Bioanalyzer (Agilent Technologies, Santa Clara, CA, USA). Then the libraries were constructed using VAHTS Universal V6 RNA-seq Library Prep Kit according to the manufacturer's instructions. The libraries were sequenced on an llumina Novaseq 6000 platform and 150 bp paired-end reads were generated. About 47.5 raw reads for each sample were generated. Raw reads of fastq format were firstly processed using fastp and the low quality reads were removed to obtain the clean reads. Then about 46.6 clean reads for each sample were retained for subsequent analyses. The clean reads were mapped to the homo sapiens using HISAT2. FPKM of each gene was calculated and the read counts of each gene were obtained by HTSeq-count. Differential expression analysis was performed using the DESeq. $P < 0.05$ and foldchange > 1.5 or foldchange < 0.67 was set as the threshold for significantly differential expression gene (DEGs).KEGG (Kyoto Encyclopedia of Genes and Genomes) pathway,GO (Gene Ontology) enrichment analysis and GSEA (Gene Set Enrichment Analysis) were performed using oeCloud(cloud.oebiotech.com).

Lactate level and Glucose measurement

Cell supernatant lactate levels were detected using a Lactate Assay Kit (Nanjing Jiancheng, China) and glucose levels were detected using GLU Assay Kit (Nanjing Jiancheng, China) according to the

manufacturer's protocol. The cell supernatant was taken at 18h and 24h treated by control,5uM 3-MA or 0.05,0.1,0.5,1,2.5 nM Rapa for measurement. Inner cell lactate levels were detected using a Lactate Concentration Assay Kit (Solarbio, China) according to the manufacturer's protocol. The data were obtained from three independent experiments.

Quantitative Real-Time Polymerase

Total RNA was extracted from the cells treated with control,5uM 3-MA or 0.5nM Rapa using Trizol (Invitrogen, CA, USA). The mRNA was reverse-transcribed to cDNA using the Tissue RNA Purification Kit Plus (EZBioscience, America) according to the manufacturer's protocol. The qRT-PCR analysis was performed with Hieff® qPCR SYBR Green Master Mix (YEASEN, China) in a Light Cycle Roche 480 II Real-time PCR system (Roche, Basel Switzerland).Three replicates were analyzed. The primer sequences used for qRT-PCR analysis are listed in Table 1. The expression levels of target genes were normalized with β-actin(internal control).

TABLE 1 | Primer sequences for qRT-PCR.

Gene	Forward primer (5′ –3′)	Reverse primer (5′ –3′)
β-actin	GGGAAATCGTGCGTGACATTAAG	TGTGTTGGCGTACAGGTCTTTG
GLUT1	CTTTGTGGCCTTCTTTGAAGT	CCACACAGTTGCTCCACAT
GLUT3	ATGCCCTACCAATATCCAGCA	GCTCCCAGTGGACTCATCTG
GLUT4	TGCTCGATTATGCACTGGAAGT	ATGAACCCCATACTCCTTCCCAG
MCT1	AAAGTGGTGAGCTGCGACGTGA	CGTTATATGCGCGGATCGCAG
MCT4	GATATGGGCGCTTACCATTTTCG	TGTGCTGCGTGACATTCCAA
PFKL	AGATGCGCACCAGCATCAACG	GAACCCGGCACATTGTTGGA
LDHA	GGAGGACCCAGCAATTAGTCT	GTTCACCCATCGCGGTTTAT
PKM2	ATGGCTGACACATTCCTGGAGC	CCTTCAACGTCTCCACTGATCG

Ldha activity measurement

Cell Ldha activity were detected using a Ldha Activity Assay Kit (Solarbio, China) according to the manufacturer's protocol. HFSCs were treated with control, 5uM 3-MA or 0.5nM Rapa for 24h,and 1 × 106 cells were collected for measurement. The data were obtained from three independent experiments.

Colony Formation Assay

The HFSCs (1 × 105 cells per well) seeded in six-well plates were treated with control, Rapa and Rapa + si-Ldha for 72h. The cells were fixed in 4% paraformaldehyde (Solarbio) for 10 min and stained with crystal violet for 10 min. Image processing was using the ImageJ/Fiji software (three pictures were analyzed). The data were obtained from three independent experiments.

Statistical Analysis

All statistical analyses were performed using the GraphPad Prism 8 software. The data are expressed as mean ± S.E.M. All data were analyzed using the Student's t-test or. A $p < 0.05$ was considered significance of difference. All treatments were repeated at least two times.

Abbreviations

-KB
-ketobutyrate
-KG
-ketoglutarate
3-MA
3-methyladenine
AGA
androgenic alopecia
CK15
cytokeratin-15
CK19
cytokeratin-19
CQ
chloroquine
H&E
hematoxylin and eosin
HFSCs
hair follicle stem cells
Ldha
lactate dehydrogenase
ORS
outer root sheath
OXPHOS
oxidative phosphorylation
PCR
polymerase chain reaction
Rapa
rapamycin
SGSCs
salivary gland stem cells
TCA
tricarboxylic acid

Declarations

Ethics approval and consent to participate

Scalp human HFs were obtained with informed, written consent of patients. All hair follicles used in this study were approved by the research ethics board at Nanfang Hospital, Southern Medical University, Guangzhou, China, following the “Declaration of Helsinki Principles”. (1)Title of the approved project : Study on the characteristics and expression profiles of hair follicles in different parts;(2)Name of the institutional approval committee or unit: Southern Medical University ; (3)Approval number : NFEC-202201-K4; (4) Date of approval : 2023-01-19 . The animal experiments were approved by the Animal Research Committee, Southern Medical University (Guangzhou, China).

Consent for publication

Not applicable; our manuscript contains no individual person’s data.

Availability of data and materials

The datasets generated and analyzed during the current study are available in the Gene Expression Omnibus repository , hyperlink to dataset in https://www.ncbi.nlm.nih.gov/geo/.

Competing interests

The authors declare that they have no competing interests.

Funding

This study was funded by the Natural Science Foundation of Guangdong Province (Title: The mechanism research by which androgen inhibits hair matrix cells autophagy and promotes apoptosis by activating the AR/miR-128-3p/TFEB pathway; Project number: Grant Nos. 2023A1515012827), the Guangdong Basic and Applied Basic Research Foundation (Title: The mechanism research by which androgen regulates endoplasmic reticulum stress and apoptosis in hair matrix cells through the AR/miR-217/Sirt1/UFM1 pathway; Project number: Grant No.2021A1515110116).

Authors' contributions

PS, ZW, SXL conducted the experiments; PS,YG and SL wrote the paper; ZL,HW were responsible for the statistical analysis; FX, QQ modified the paper; ZH,KL, and YM designed and guide the experiments. All authors read and approved the final manuscript.

Acknowledgements

We would like to express our sincere thanks to Guangdong Provincial Key Laboratory of Construction and Detection in Tissue Engineering for providing experimental instruments.

Authors' information (optional)

PS(sunnnnp@163.com), ZW(1486619689@qq.com), SXL(1146434696@qq.com), SL(woshi17438@163.com), YG(gyy1103@smu.edu.cn),ZL(linzhen@smu.edu.cn), HW(wanghailin_12@163.com), FX(13268266265@163.com), QQ(15521263230@163.com), ZH(huzhiqidr163@i.smu.edu.cn), TL(likaitao13@smu.edu.cn), YM(miaoyong123@i.smu.edu.cn)

References

1. Hsu YC, Pasolli HA, Fuchs E. Dynamics between stem cells, niche, and progeny in the hair follicle. Cell. 2011;144:92–105.
2. Mokry J, Pisal R. Development and Maintenance of Epidermal Stem Cells in Skin Adnexa. Int J Mol Sci. 2020;21.
3. Choi S, Zhang B, Ma S, Gonzalez-Celeiro M, Stein D, Jin X, et al. Corticosterone inhibits GAS6 to govern hair follicle stem-cell quiescence. Nature. 2021;592:428–32.
4. Garza LA, Yang CC, Zhao T, Blatt HB, Lee M, He H, et al. Bald scalp in men with androgenetic alopecia retains hair follicle stem cells but lacks CD200-rich and CD34-positive hair follicle progenitor cells. J Clin Invest. 2011;121:613–22.
5. Flores A, Schell J, Krall AS, Jelinek D, Miranda M, Grigorian M, et al. Lactate dehydrogenase activity drives hair follicle stem cell activation. Nat Cell Biol. 2017;19:1017–26.
6. Kim CS, Ding X, Allmeroth K, Biggs LC, Kolenc OI, L'Hoest N, et al. Glutamine Metabolism Controls Stem Cell Fate Reversibility and Long-Term Maintenance in the Hair Follicle. Cell Metab. 2020;32:629–42.
7. Orhon I, Rocchi C, Villarejo-Zori B, Serrano MP, Baanstra M, Brouwer U, et al. Autophagy induction during stem cell activation plays a key role in salivary gland self-renewal. Autophagy. 2022;18:293–308.
8. Ho TT, Warr MR, Adelman ER, Lansinger OM, Flach J, Verovskaya EV, et al. Autophagy maintains the metabolism and function of young and old stem cells. Nature. 2017;543:205–10.
9. Chai M, Jiang M, Vergnes L, Fu X, de Barros SC, Doan NB, et al. Stimulation of Hair Growth by Small Molecules that Activate Autophagy. Cell Rep. 2019;27:3413–21.
10. Parodi C, Hardman JA, Allavena G, Marotta R, Catelani T, Bertolini M, et al. Autophagy is essential for maintaining the growth of a human (mini-)organ: Evidence from scalp hair follicle organ culture. Plos Biol. 2018;16:e2002864.
11. Paus R, Handjiski B, Czarnetzki BM, Eichmüller S. A murine model for inducing and manipulating hair follicle regression (catagen): effects of dexamethasone and cyclosporin A. J Invest Dermatol. 1994;103:143–7.
12. Dong S, Wang Q, Kao YR, Diaz A, Tasset I, Kaushik S, et al. Chaperone-mediated autophagy sustains haematopoietic stem-cell function. Nature. 2021;591:117–23.
13. Wen L, Miao Y, Fan Z, Zhang J, Guo Y, Dai D, et al. Establishment of an Efficient Primary Culture System for Human Hair Follicle Stem Cells Using the Rho-Associated Protein Kinase Inhibitor Y-

27632. Front Cell Dev Biol. 2021;9:632882.
14. Fan Q, Yang L, Zhang X, Ma Y, Li Y, Dong L, et al. Autophagy promotes metastasis and glycolysis by upregulating MCT1 expression and Wnt/β-catenin signaling pathway activation in hepatocellular carcinoma cells. J Exp Clin Canc Res. 2018;37:9.
15. Li T, Tong H, Yin H, Luo Y, Zhu J, Qin Z, et al. Starvation induced autophagy promotes the progression of bladder cancer by LDHA mediated metabolic reprogramming. Cancer Cell Int. 2021;21:597.
16. Sotthibundhu A, Promjuntuek W, Liu M, Shen S, Noisa P. Roles of autophagy in controlling stem cell identity: a perspective of self-renewal and differentiation. Cell Tissue Res. 2018;374:205–16.
17. Gund R, Christiano AM. Impaired autophagy promotes hair loss in the C3H/HeJ mouse model of alopecia areata. Autophagy. 2023;19:296–305.
18. Kim KH, Lee MS. Autophagy–a key player in cellular and body metabolism. Nat Rev Endocrinol. 2014;10:322–37.
19. Morinaga H, Mohri Y, Grachtchouk M, Asakawa K, Matsumura H, Oshima M, et al. Obesity accelerates hair thinning by stem cell-centric converging mechanisms. Nature. 2021;595:266–71.
20. Li YF, Ouyang SH, Tu LF, Wang X, Yuan WL, Wang GE, et al. Caffeine Protects Skin from Oxidative Stress-Induced Senescence through the Activation of Autophagy. Theranostics. 2018;8:5713–30.
21. Rossiter H, Stübiger G, Gröger M, König U, Gruber F, Sukseree S, et al. Inactivation of autophagy leads to changes in sebaceous gland morphology and function. Exp Dermatol. 2018;27:1142–51.

Figures

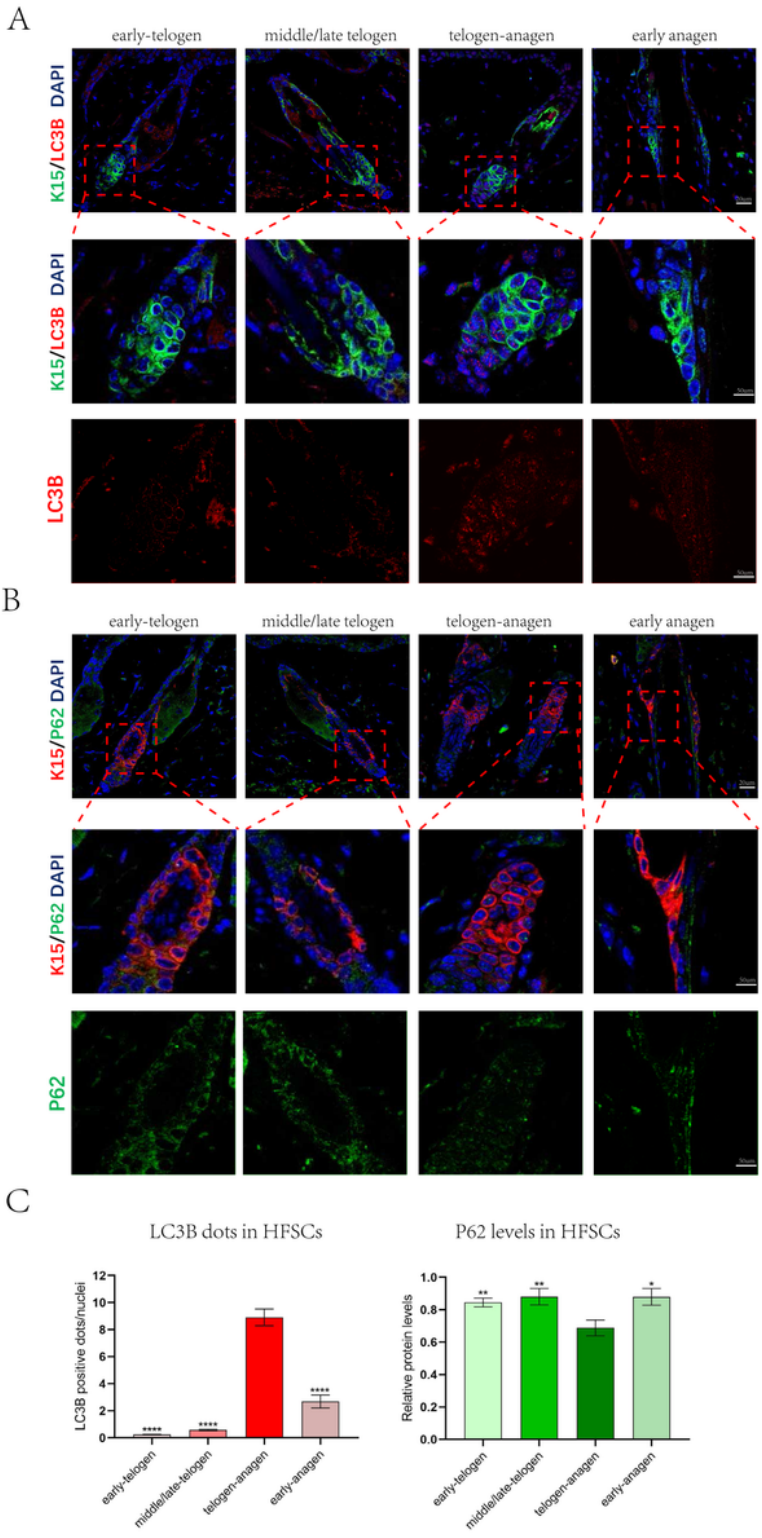

Figure 1

Autophagy is enhanced during the transition from telogen to anagen. (**A**) Representative immunostaining images of dorsal hair follicles stained with anti-LC3B(red) and anti-K15 antibodies(green) in early telogen, middle/late telogen, telogen-anagen transition and anagen phase. (**B**) Representative immunostaining images of dorsal hair follicles stained with anti-P62(green) and anti-K15 antibodies(red) in early telogen, middle/late telogen, telogen-anagen transition and anagen phase. (**C**) Quantification of LC3B-fluorescent

dots/cell in K15+HFSCs region of dorsal hair follicles(left);Quantification of P62-fluorescent signal in K15+HFSCs region of hair follicles(right).The data represent the means±S.E.M from at least three independent experiments. *P < 0.05, **P < 0.01, ****P < 0.0001,determined by Student's t-test.

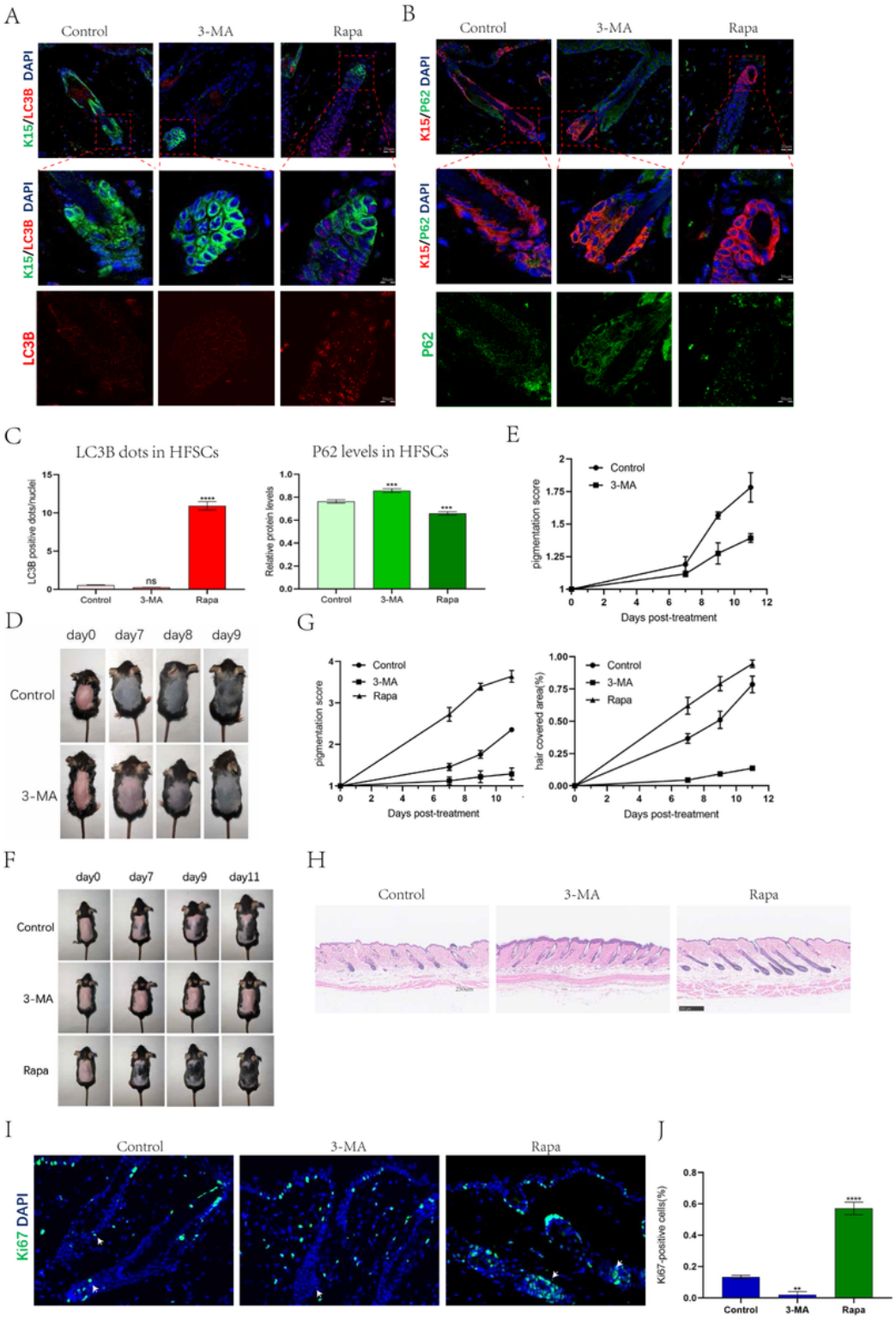

Figure 2

Autophagy affects mice hair follicle cycle and HFSC activation. (**A**) Representative immunostaining images of dorsal hair follicles treated with control,3-MA(24h) or Rapa(24h) stained with anti-LC3B(red) and anti-K15 antibodies(green).(**B**) Representative immunostaining images of dorsal hair follicles treated with control,3-MA(24h) or Rapa(24h) stained with anti-P62(green) and anti-K15 antibodies(red).(**C**) Quantification of LC3B-fluorescent dots/cell in K15+HFSCs region of control,3-MA-treated or Rapa-treated hair follicles(left);Quantification of P62-fluorescent signal in K15+HFSCs region of control,3-MA-treated or Rapa-treated hair follicles(right);(**D**) Inhibited autophagy inhibits hair regeneration.C57BL/6 mice were shaved on postnatal week 8-9 and topically treated with control or 3-MA every other day. Photographs were taken on day 7,9,11 post-treatment.(**E**) Quantification for appearance of melanin pigmentation in dorsal skin.(**F**) Enhanced autophagy induces hair regeneration.C57BL/6 mice were shaved on postnatal week 8-9 and topically treated with control, 3-MA or Rapa every other day. Photographs were taken on day 7,9,11 post-treatment.(**G**) Quantification for appearance of melanin pigmentation and hair covered area in dorsal skin.(**H**) Microphotographs of H&E stained skin tissue section from mice treated with control, 3-MA or Rapa.(**I and J**) Rapa increases Ki67+ HFSCs (white arrow).(**I**) Microphotographs of Ki67 stained skin tissue section from mice treated with control,3-MA or Rapa.(**J**) Quantification for Ki67+HFSCs numbers in dorsal hair follicle .The data represent the means± S.E.M from at least three independent experiments. **P < 0.01,***P < 0.001,****P < 0.0001,determined by Student’s t-test.

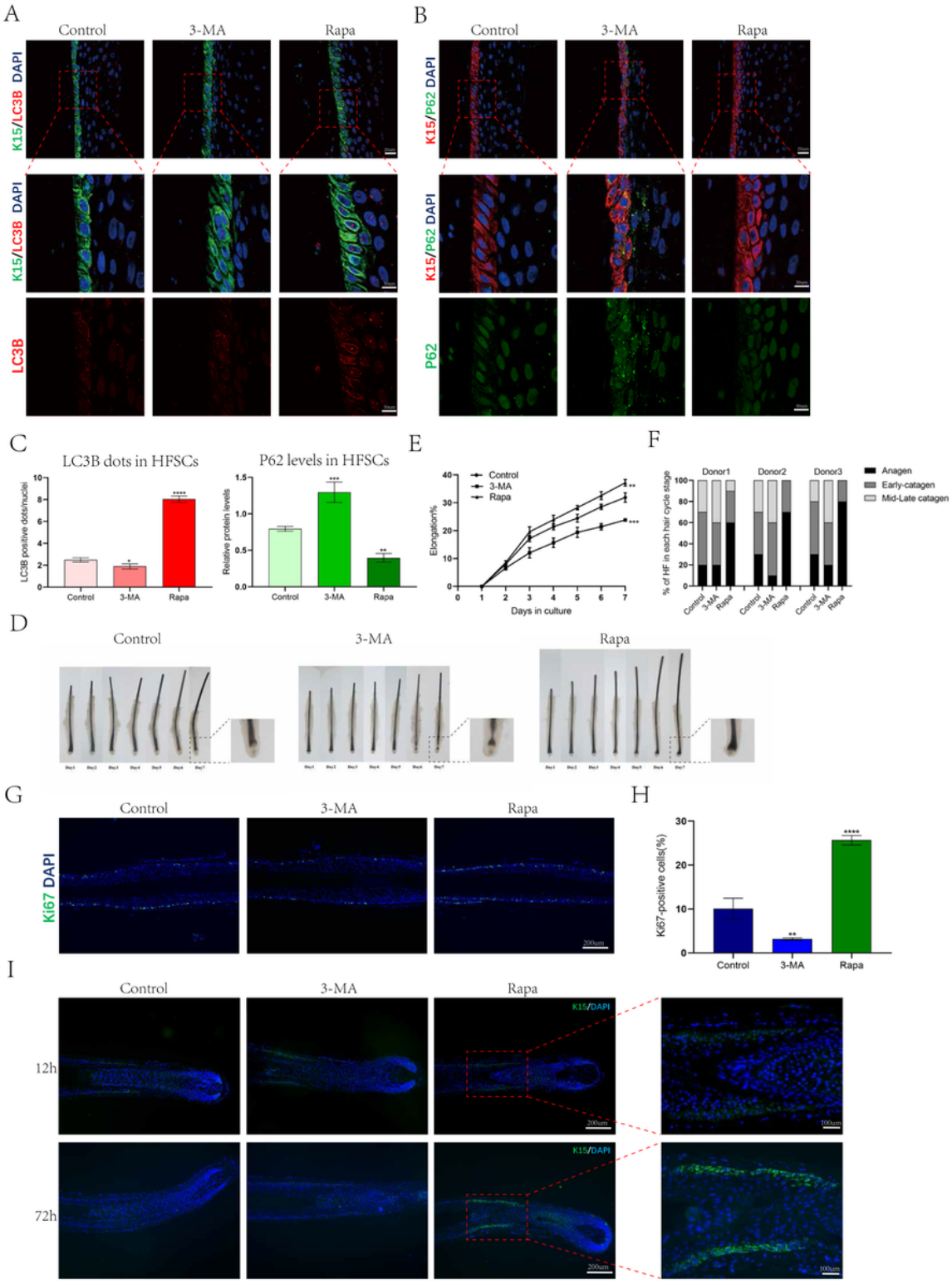

Figure 3

Autophagy affects human hair follicle and HFSC activation.(**A**) Representative immunostaining images of human hair follicles treated with control,3-MA(8h) or Rapa(8h) stained with anti-LC3B(red) and anti-K15 antibodies(green).(**B**) Representative immunostaining images of dorsal hair follicles treated with control,3-MA(8h) or Rapa(8h) stained with anti-P62(green) and anti-K15 antibodies(red).(**C**) Quantification of LC3B-fluorescent dots/cell in K15+HFSCs region of control,3-MA-treated or Rapa-treated

hair follicles(left);Quantification of P62-fluorescent signal in K15+HFSCs region of control,3-MA-treated or Rapa-treated hair follicles(right).(**D**) Human hair follicles were treated with control,3-MA or Rapa .Photographs were taken for 7 consecutive days.(**E**) Increased hair shaft elongation after Rapa treatment. Independent experiments were repeated at least three times and data is based on 30 hair follicles from three donors. (**F**) Quantification of hair cycle stages of cultured hair follicles treated with control,3-MA or Rapa. (**G and H**) Rapa promotes HFSC activation. (**G**) The proliferative HFSCs were assessed by the proliferative marker, Ki67 (green) on post-treatment day 3.(**H**) Quantification of Ki67+cells of control,3-MA-treated or Rapa-treated hair follicles.(**I**) Representative immunostaining images of human hair follicles treated with control,3-MA or Rapa stained with anti-K15 antibodies(green) on 12h and 72h post-treatment. The data represent the means± S.E.M. from at least three independent experiments. *P < 0.05,**P < 0.01, ***P < 0.001,****P < 0.0001,determined by Student's t-test.

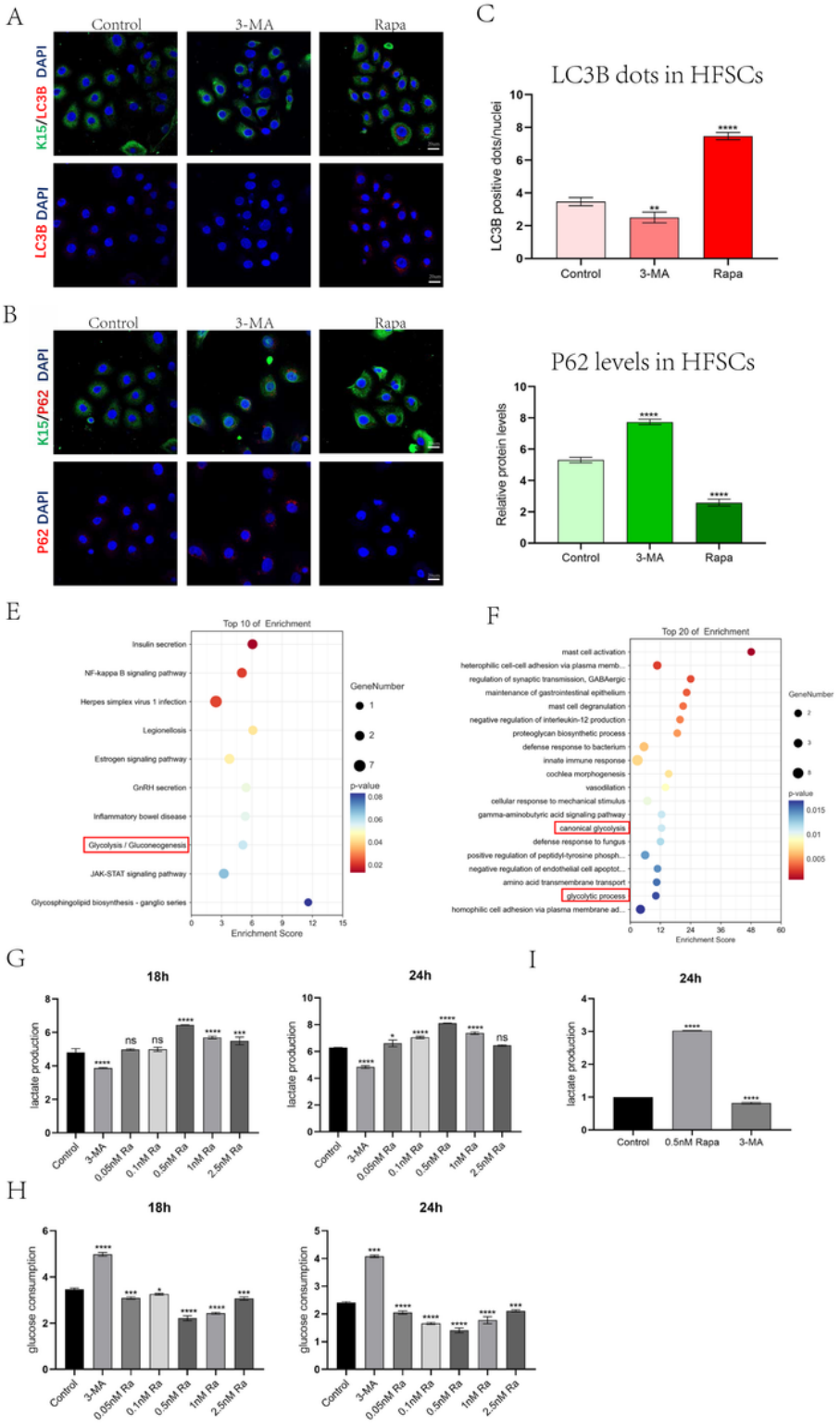

Figure 4

Autophagy promoted HFSC glycolysis.(**A**) Representative immunostaining images of human hair follicles treated with control,3-MA(6h) or Rapa(6h) stained with anti-LC3B(red) and anti-K15 antibodies(green).(**B**) Representative immunostaining images of dorsal hair follicles treated with control,3-MA(6h) or Rapa(6h) stained with anti-P62(red) and anti-K15 antibodies(green). (**C**) Quantification of LC3B-fluorescent dots/cell of control,3-MA-treated or Rapa-treated HFSCs(up); Quantification of P62-fluorescent signal of

control,3-MA-treated or Rapa-treated HFSCs(down). (**D**) KEGG pathway enrichment analysis bubble chart. (**E**) Biological process category enrichment bubble chart of GO analysis. The Y-axis of the bubble chart represents GO or KEGG pathway terms, and the color of the bubble represents the P value of the terms.(**F and G**) Analysis of the consumption of glucose and production of lactate in HFSCs supernatant cultured with control, 3-MA or different concentrations of Rapa for 18h and 24h.(**H**) Analysis of the production of lactate in HFSCs cultured with control, 3-MA or Rapa(0.5nM) for 24h.The data represent the means± S.E.M. from at least three independent experiments. *P < 0.05,**P < 0.01, ***P < 0.001,****P < 0.0001,determined by Student's t-test.

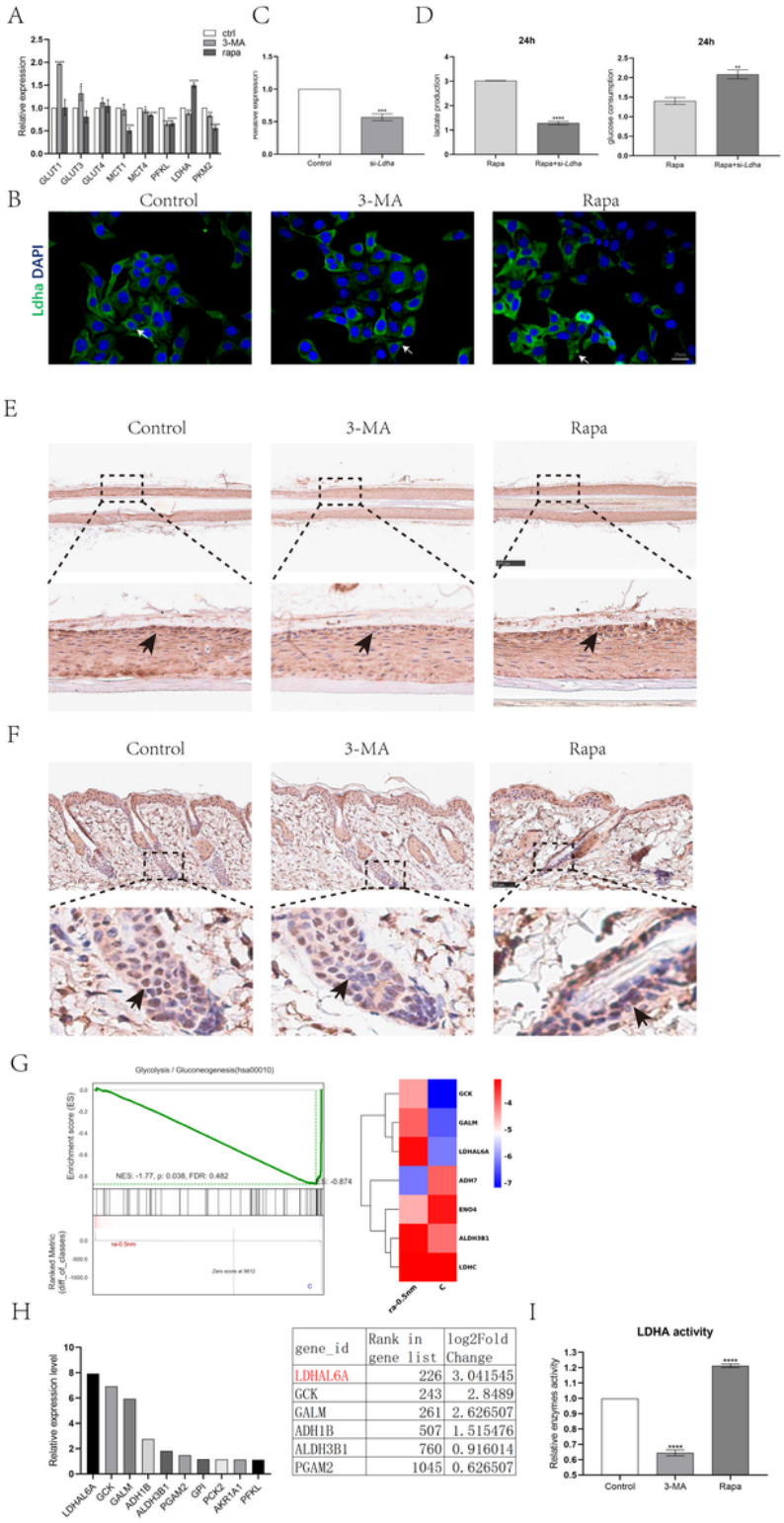

gene_id	Rank in gene list	log2Fold Change
LDHAL6A	226	3.041545
GCK	243	2.8489
GALM	261	2.626507
ADH1B	507	1.515476
ALDH3B1	760	0.916014
PGAM2	1045	0.626507

Figure 5

Autophagy promoted HFSC glycolysis by upregulating Ldha and increasing Ldha activity. (**A and B**) The expression levels of glycolysis key enzymes in HFSCs cultured with control, 3-MA or Rapa for 24h were detected by real-time PCR and immunofluorescence.(**C**) Real-time PCR was used to examine the expression of Ldha in HFSCs transfected with Ldha siRNA. (**D**) Analysis of the consumption of glucose and production of lactate in HFSCs supernatant cultured with Rapa for 24h after transfected with Ldha

siRNA.(**E and F**) Rapa promotes Ldha expression in vitro and in vivo.(**E**) Representative immunohistochemical images of human hair follicles treated with control,3-MA(24h) or Rapa(24h) stained with anti-Ldha antibodies.(**F**) Representative immunohistochemical images of dorsal hair follicles treated with control,3-MA(24h) or Rapa(24h) stained with anti-Ldha antibodies.(**G**) Gene set enrichment analysis (GSEA) on RNA-seq transcriptome data from HFSCs treated with control or Rapa shows enrichment for glycolysis/gluconeogenesis pathway (left) and the gene signature (right), with LDHAL6A as the top up-regulated gene.(**H**) Fold change of TE for glycolytic genes between Rapa-treated HFSCs and control HFSCs.(**I**) Relative Ldha activity in HFSCs treated with control,3-MA(24h) or Rapa(24h).The data represent the means± s.e.m from at least three independent experiments.*P < 0.05,**P < 0.01, ***P < 0.001,****P < 0.0001,determined by Student's t-test.

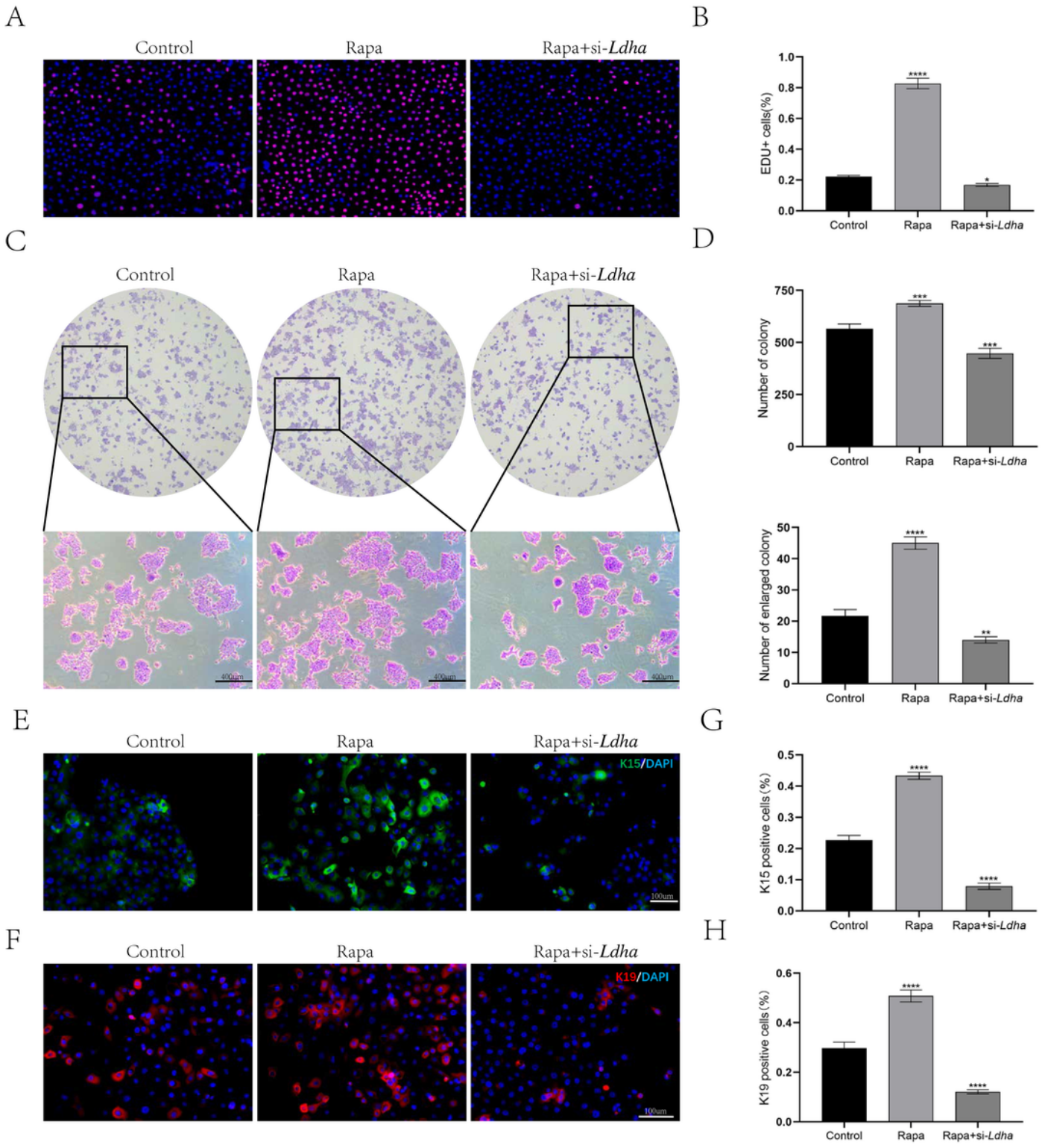

Figure 6

Autophagy-induced glycolysis promoted proliferation and maintained the stemness of HFSCs. (**A**) HFSCs treated with control, Rapa or Rapa+si-Ldha were subjected to the EdU labeling assay (EdU-positive (red); Hoechst (blue)). (**B**) Quantification of the proportion of EdU-positive cells in control, Rapa-treated or Rapa+si-Ldha-treated group. (**C**) Colony formation assays further confirmed that Rapa increased the proliferation of HFSCs and si-Ldha impaired Rapa-induced proliferation. (**D**) Quantification of clone-

forming colony number(up) and large colonies(>100 cells/colony, down). (**E and F**) Immunofluorescence staining with anti-K15 antibodies or anti-K19 antibodies of HFSCs treated with control, Rapa or Rapa+si-Ldha was performed on day 3 of culturing. (**G and H**) Quantification of K15+cells or K19+cells of control, Rapa-treated or Rapa+si-Ldha-treated HFSCs. The data represent the means± S.E.M from at least three independent experiments. *P < 0.05,**P < 0.01, ***P < 0.001,****P < 0.0001,determined by Student's t-test.

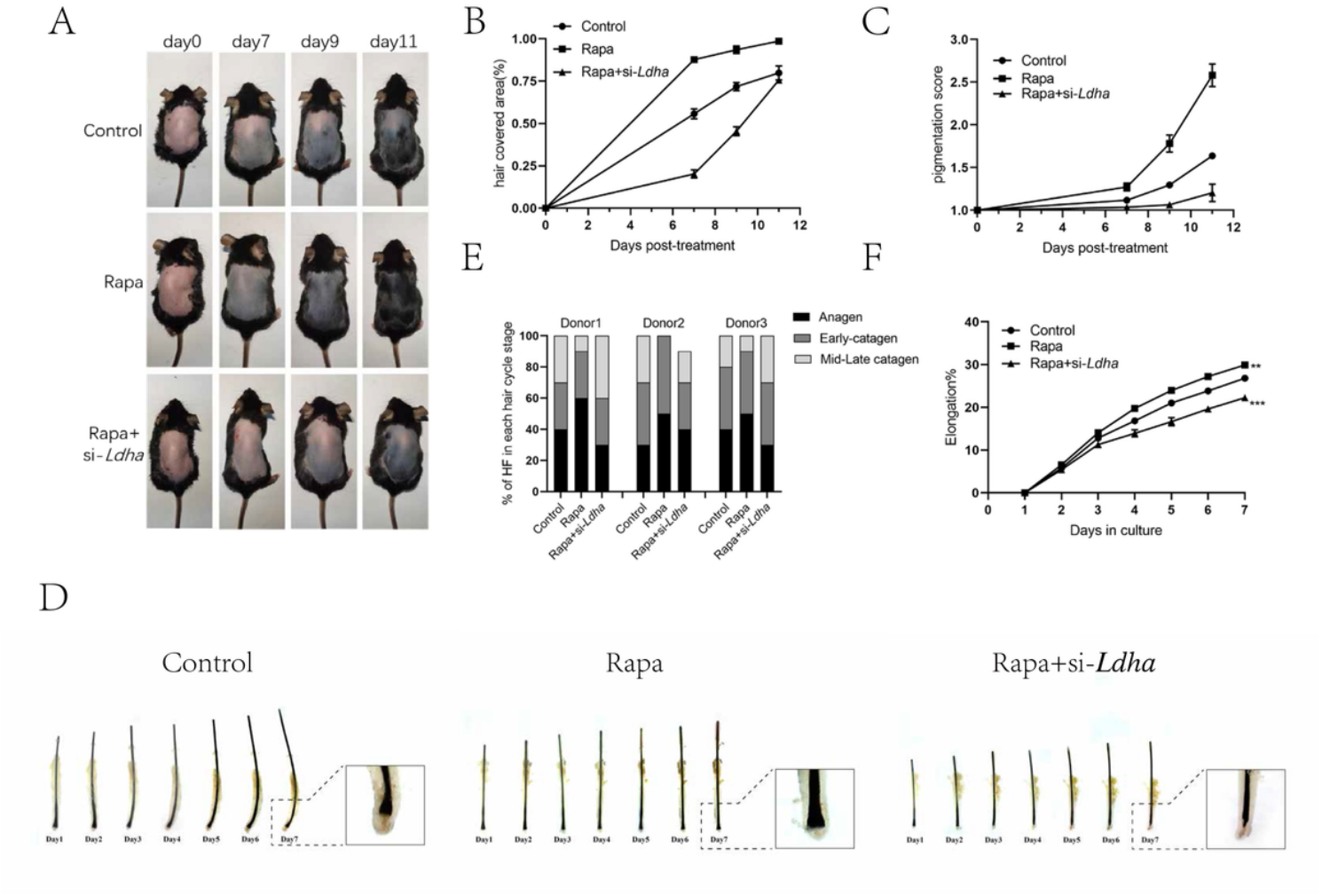

Figure 7

Autophagy-induced glycolysis regulates the hair follicle cycle. (**A**) C57BL/6 mice were shaved on postnatal week 8-9 and topically treated with control, Rapa or Rapa+si-Ldha every other day. Photographs were taken on day 7,9,11 post-treatment. (**B and C**) Quantification for appearance of melanin pigmentation and hair covered area in dorsal skin. (**D**) Human hair follicle were treated with control, Rapa or Rapa+si-Ldha. Photographs were taken for 7 consecutive days.(**E and F**) Quantification of hair cycle stages and hair shaft elongation of cultured hair follicles treated with control, Rapa or Rapa+si-Ldha.

Supplementary Files

This is a list of supplementary files associated with this preprint. Click to download.

- SupplementaryFig1.pdf
- SupplementaryFig2.pdf
- SupplementaryFig3.pdf